Numerical simulations and rheometry measurements of reception properties of Solar Orbiter RPW electric antennas.

M. Panchenko[1], G. Fischer[1] and W. Macher[1]

(1) Space Research Institute, Austrian Academy of Sciences, Graz, Austria

RPW antennas

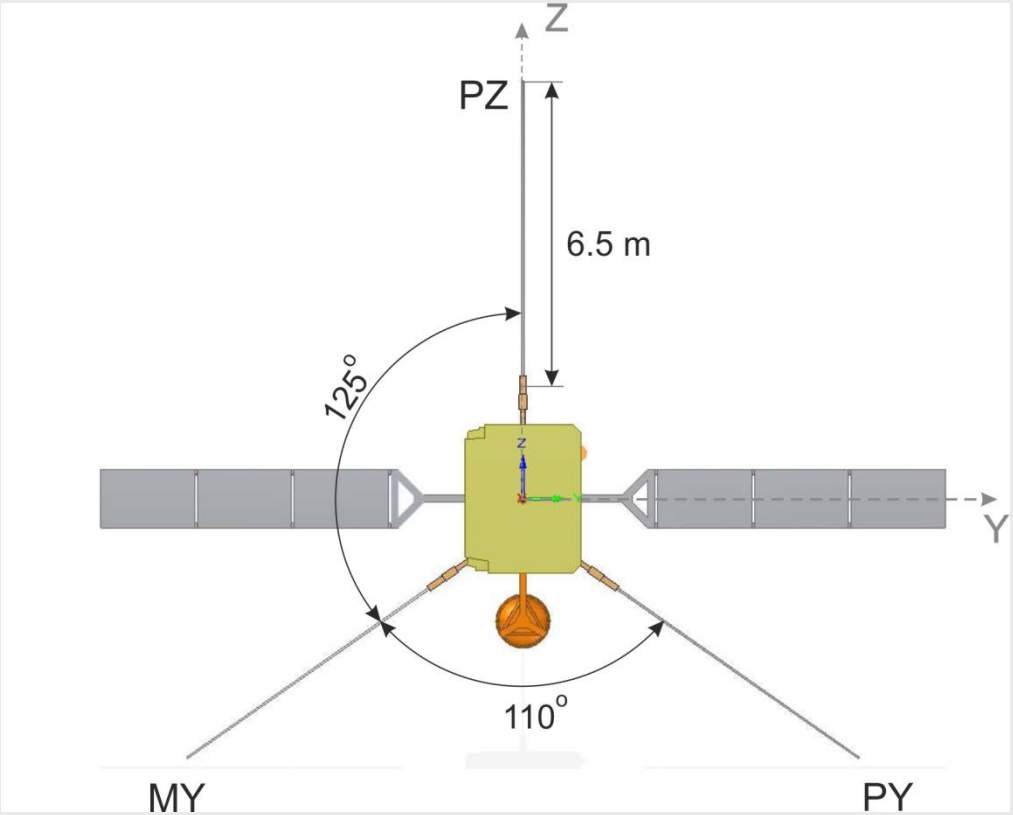

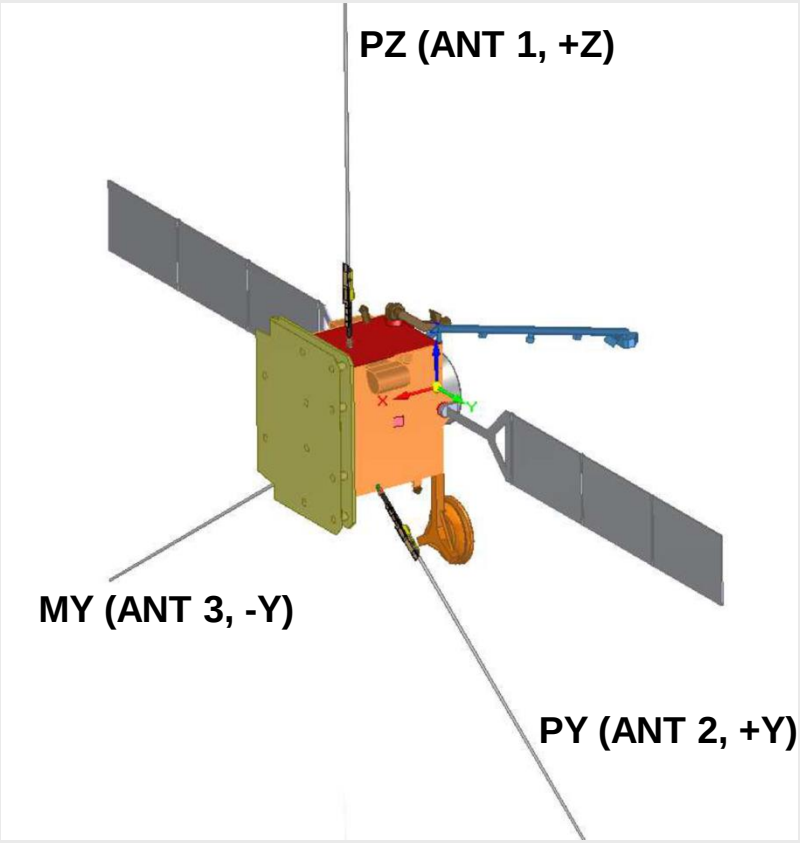

RPW electric sensors consist of three antennas PZ (ANT 1, or +Z), PY (ANT 2, or +Y) and MY (ANT 3, or -Y) mounted on booms.

RPW antennas

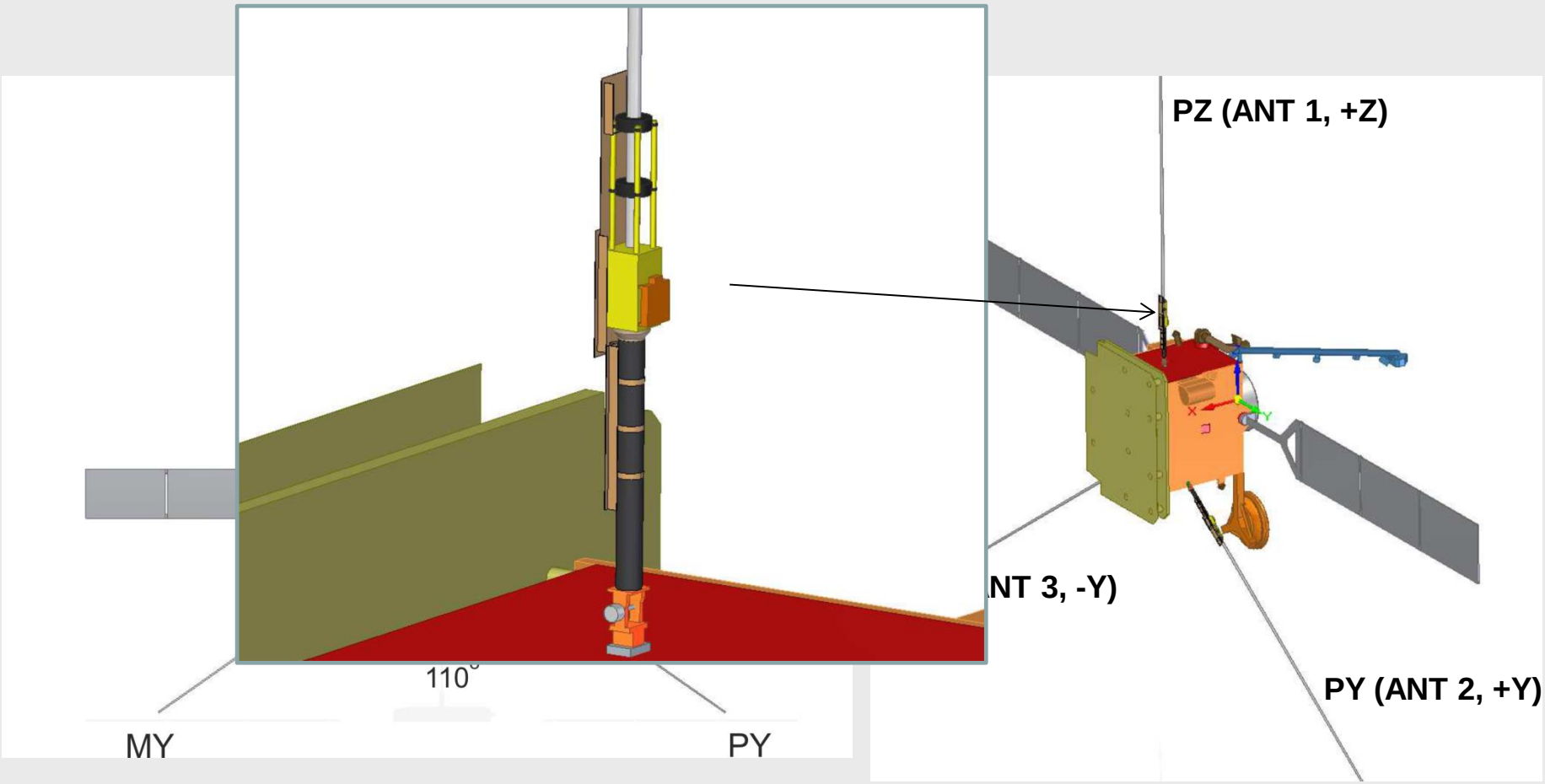

RPW electric sensors consist of three antennas PZ (ANT 1, or +Z), PY (ANT 2, or +Y) and MY (ANT 3, or -Y) mounted on booms.

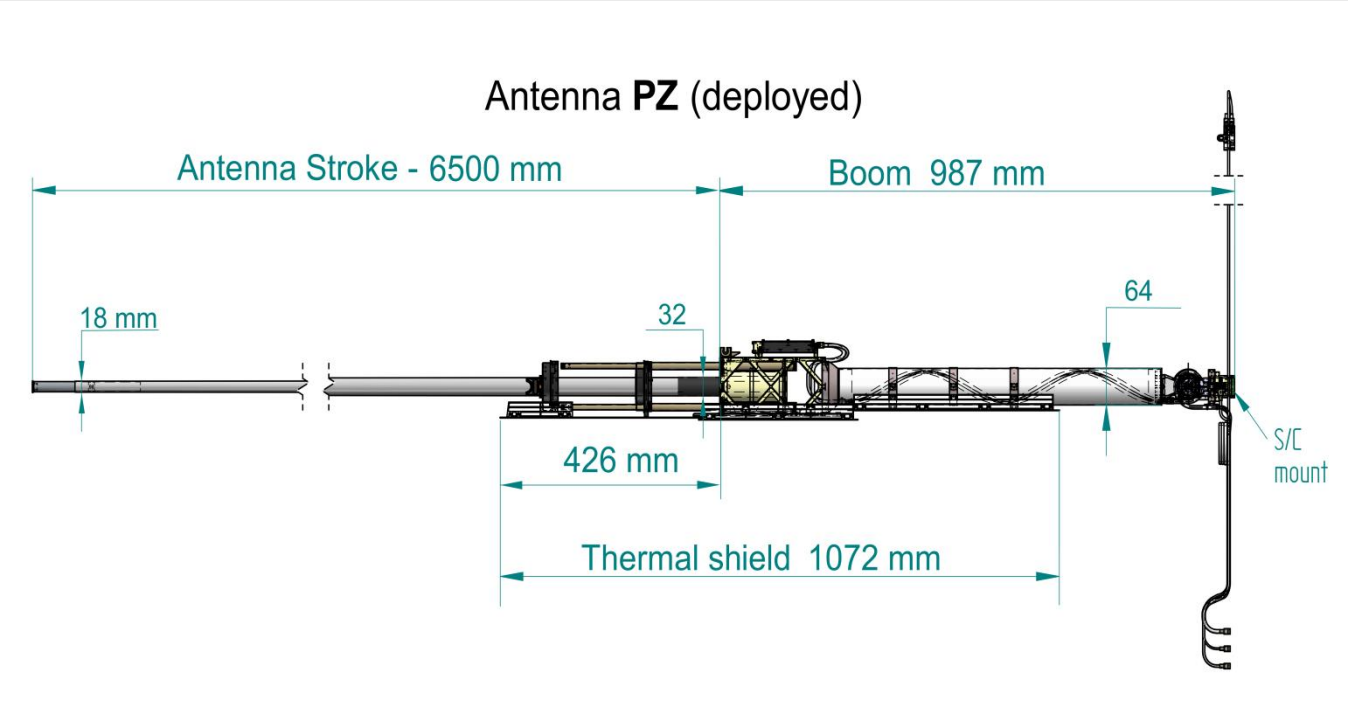

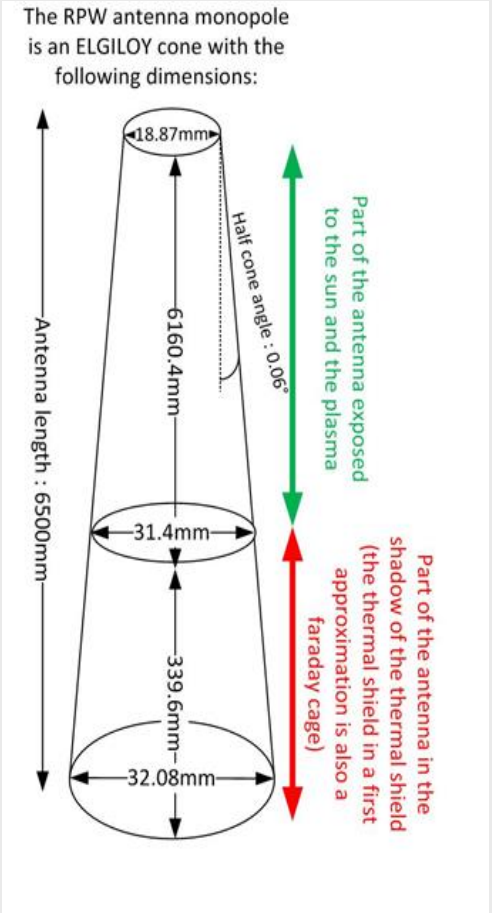

Design of deployed PZ antenna. The antenna system consists of deploying mechanism, ~1 m boom, and 6.5 m length antenna stroke. Additionally, there are thermal shields in form of niobium plates.

Reference coordinate system

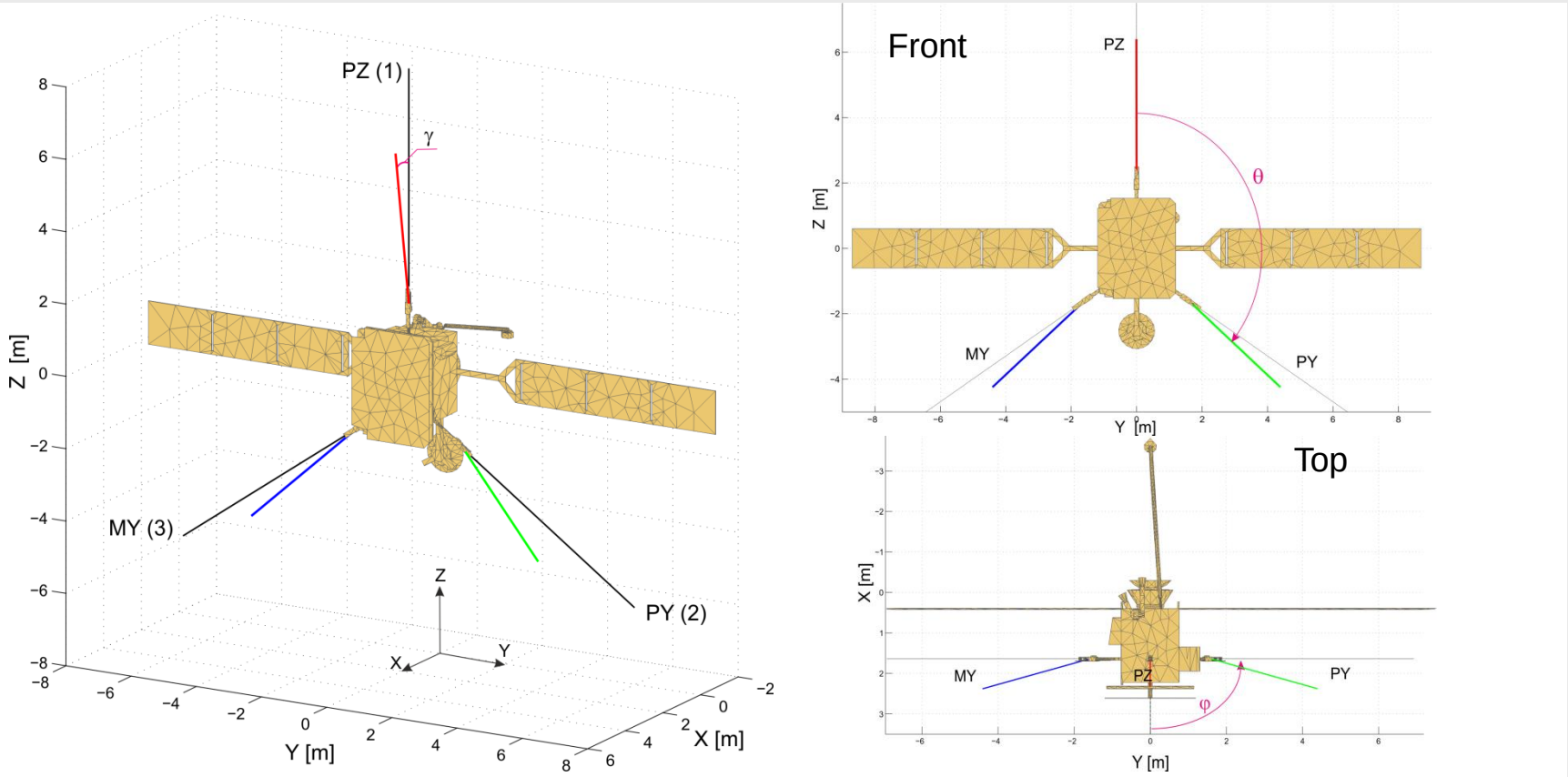

- The position of each antenna is described in s/c spherical coordinates by colatitude angle θ and azimuth angle φ and the lengths **h.**
- The colatitude θ is defined with respect to the Z spacecraft axis and azimuth φ is defined in the XY spacecraft plane starting at the X-axis.
- Angle γ describes the angular offset of the effective antenna vector with respect to the physical position of the antenna

Reference coordinate system

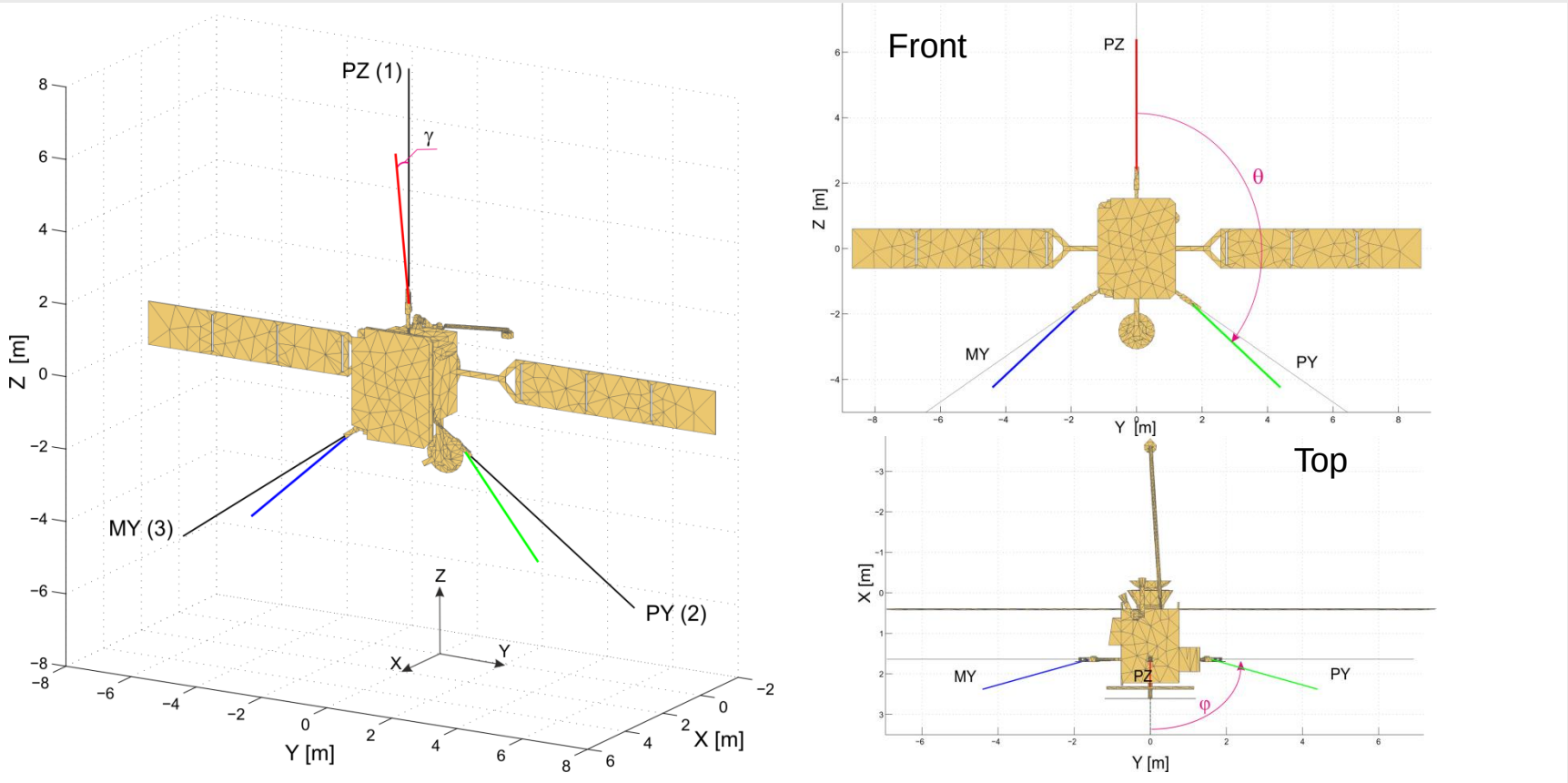

ANT	Mechanical antennas		
	h, m	θ, deg	φ, deg
PZ	6.5	0.0	0.0
PY	6.5	125	90
MY	6.5	125	-90

1. Numerical simulations using FEKO

- The conducting spacecraft body is electromagnetically coupled to the antennas and, therefore, the antenna receiving properties strongly depend on the spacecraft shape.

- The numerical simulations of the Solar Orbiter/RPW antennas was based on a reduced CAD model of the spacecraft and FEKO antenna simulation software.

- FEKO is a commercial antenna simulation tool based on the solution of the electric field integral equation. This program package includes time-frequency electromagnetic domain solvers, 3D Parasolid CAD modelling interface (CADFEKO) and comprehensive post-processing and visualization tool POSTFEKO.

Spacecraft surface-mesh modelling

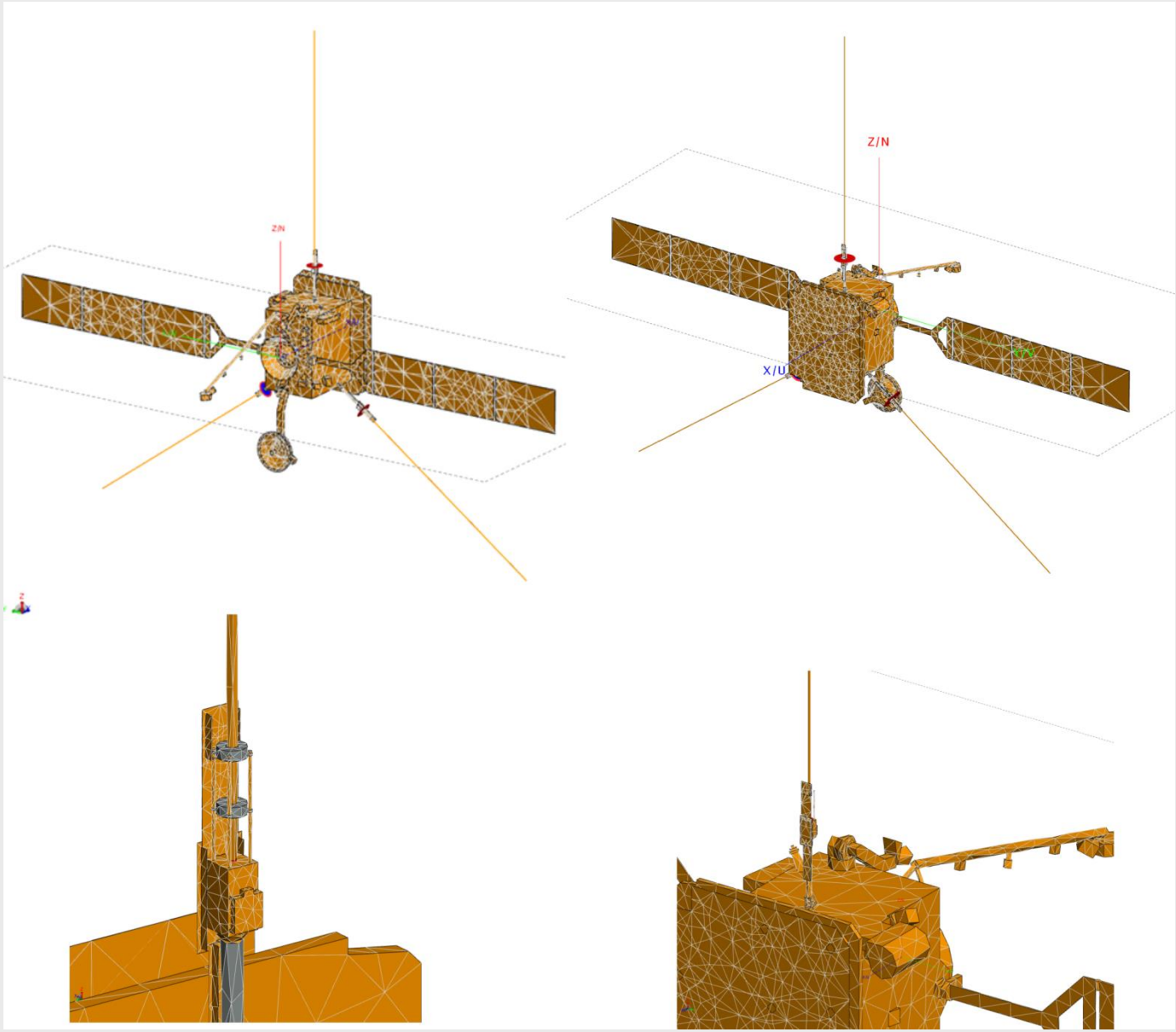

- The model consisted of about 9000 triangles and 1950 curvilinear segments.
- The current distribution of the antenna-spacecraft system calculated by FEKO has been used to define the antenna reception properties

Effective length vectors

- The open-circuit voltages on each short electrical dipole (or input voltages at each receiver channel) can be expressed as:

$$V_i = \boldsymbol{h}_i \cdot \boldsymbol{E} \qquad (1)$$

where $\boldsymbol{h}_i$ is an effective antenna length vector, $\boldsymbol{E}$ is the electric wave vector of the incoming wave and i denotes the antenna. The effective vector of the antenna represents the electrically effective direction and length of each antenna, in contrast to the physical (mechanical) antenna.

- The open port effective length vector of each antenna is given by the equation:

$$\boldsymbol{h}_i^o = \frac{1}{I_i} \int \boldsymbol{I}(\boldsymbol{r}) ds \qquad (2)$$

where I_i is the current at the feed of the i-th antenna, $\boldsymbol{I}(\boldsymbol{r})$ is the induced current distribution and *ds* is the infinitesimal line element along the respective wire segment. The integral runs over all segments of the wire grid.

Quasi-static results

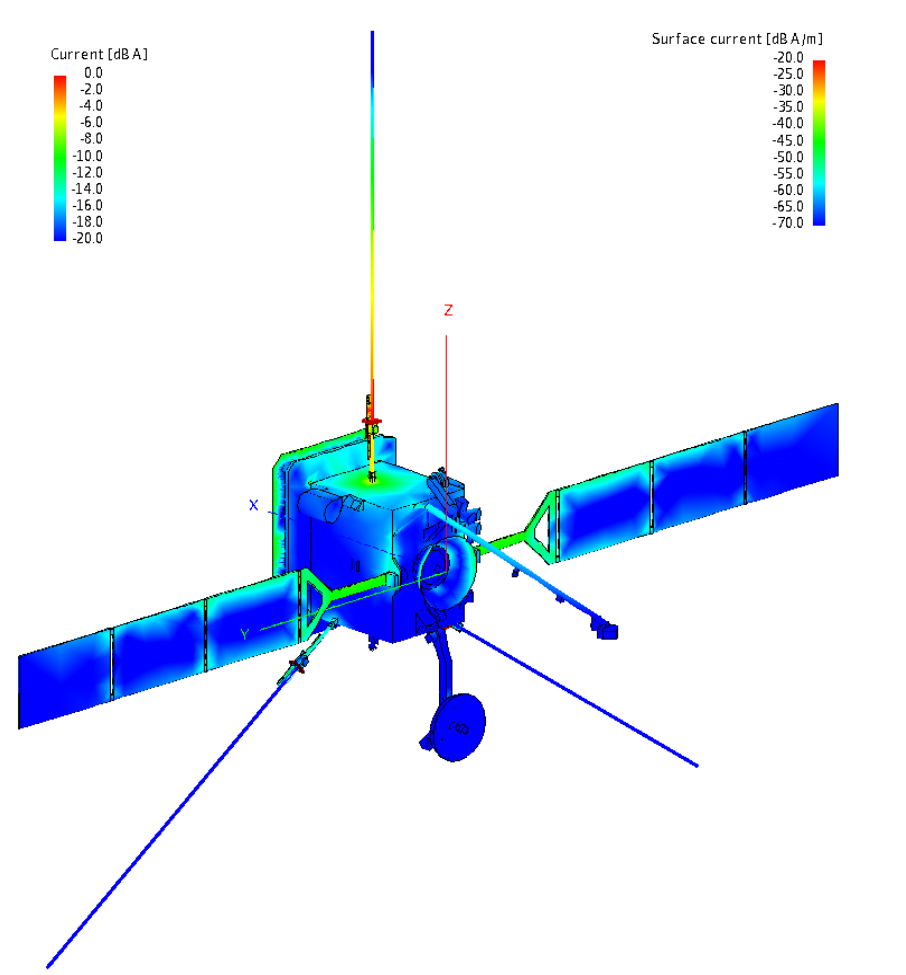

Surface currents [dB A/m] and line currents [dB A] for the Solar Orbiter model with antenna PZ driven with 1V at 300 kHz. The currents are normalized values. Feed zone of the PZ antenna have a high current density.

Quasi-static results

- Although the effective antenna vector is a complex quantity, in quasi-static frequency range, $L_{ant} \ll \lambda_{wave}$, $\boldsymbol{h}_i$ is real (imaginary part is negligible) and constant (independent of direction).

- The first simulations have been performed for quasi-static frequency range i.e. at 300 kHz. We have retrieved the effective length vectors of the antennas (length and directions) for open feeds

Quasi-static results (at 300 kHz): open ports

- The open port effective length vectors represent the reception properties of the bare antenna system without taking into account a total base capacitance composed of receiver input impedances and capacities of cable and antenna mounting structures. It is assumed that the preamplifiers or receivers connected to the antennas have very high input impedances.

ANT	Mechanical antennas			Effective antenna vectors			
	h, m	θ, deg	φ, deg	h_e, m	θ, deg	φ, deg	γ, deg
PZ	6.5	0.0	0.0	4.41	9.1	-0.4	9.1
PY	6.5	125	90	3.91	132.2	75.2	13.6
MY	6.5	125	-90	3.91	132.3	-75.2	13.6
	Pseudo-dipoles			Effective vectors of dipoles			
Dip. PZ-PY	11.53	152.5	90	7.53	158.1	-90.9	5.6
Dip. PY-MY	10.65	90.0	90	5.60	90.00	90.0	0.0
Dip. MY-PZ	11.53	152.5	-90	7.53	158.2	-89.1	5.6

Effective length vectors of PZ, PY and MY monopoles and PZ-PY, PY-MY and MY-PZ dipoles compared with physical position of the RPW antennas for open ports. h is antenna length, θ is colatitude and φ is azimuth angle. The angle γ is the angular separation between effective antenna vector and real antenna rod. The pseudo dipoles mean the vectors calculated as differences between corresponding monopoles forming the dipoles. The effective vectors of the dipoles have been calculated from the effective vectors of the corresponding monopoles.

Quasi-static results: open ports

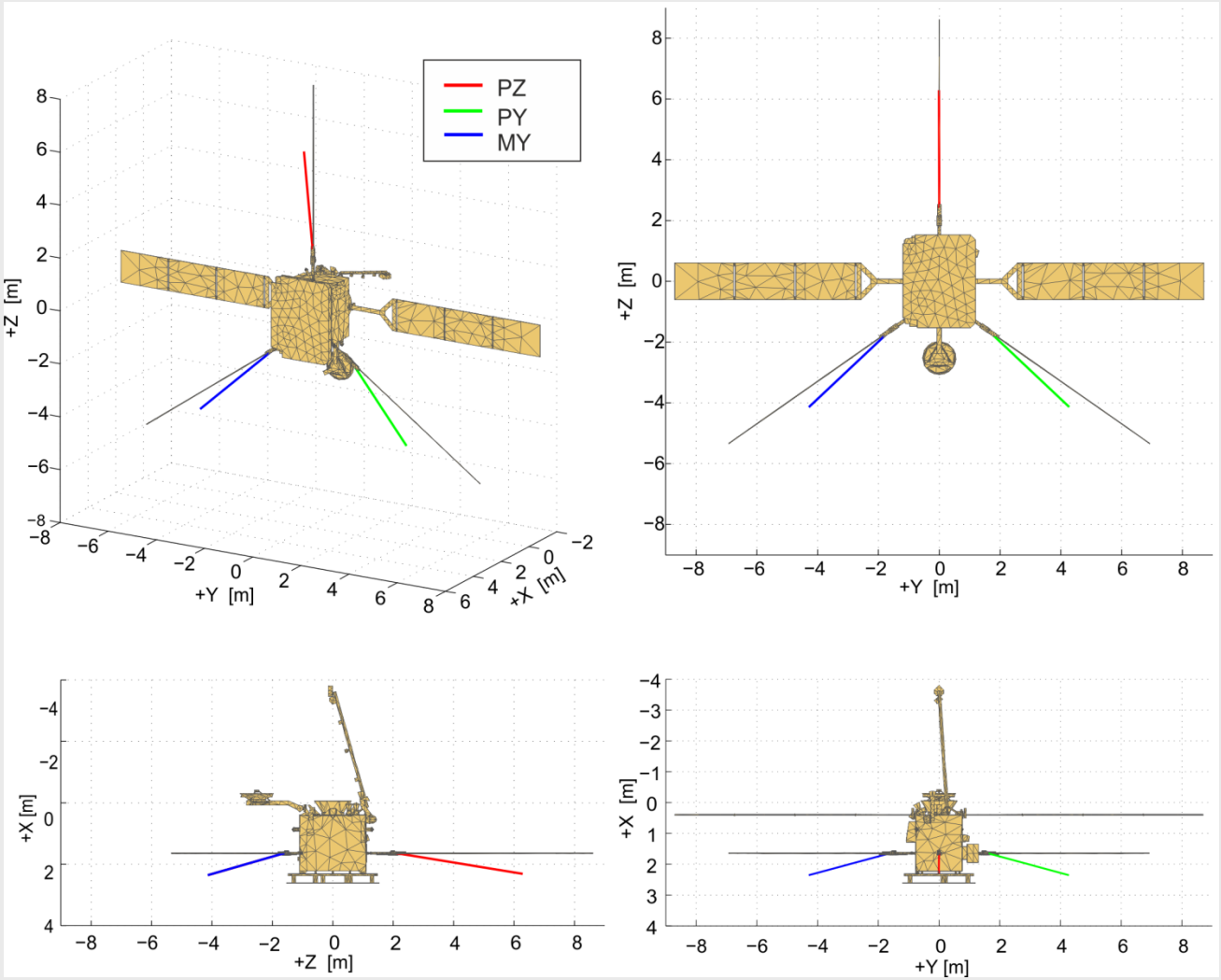

Effective length vectors at 300 kHz for a monopole configuration. Real antennas are given in black while the effective vectors are drawn in color. This gives an impression of the difference between mechanical and electrical quantities.

Quasi-static results: open ports

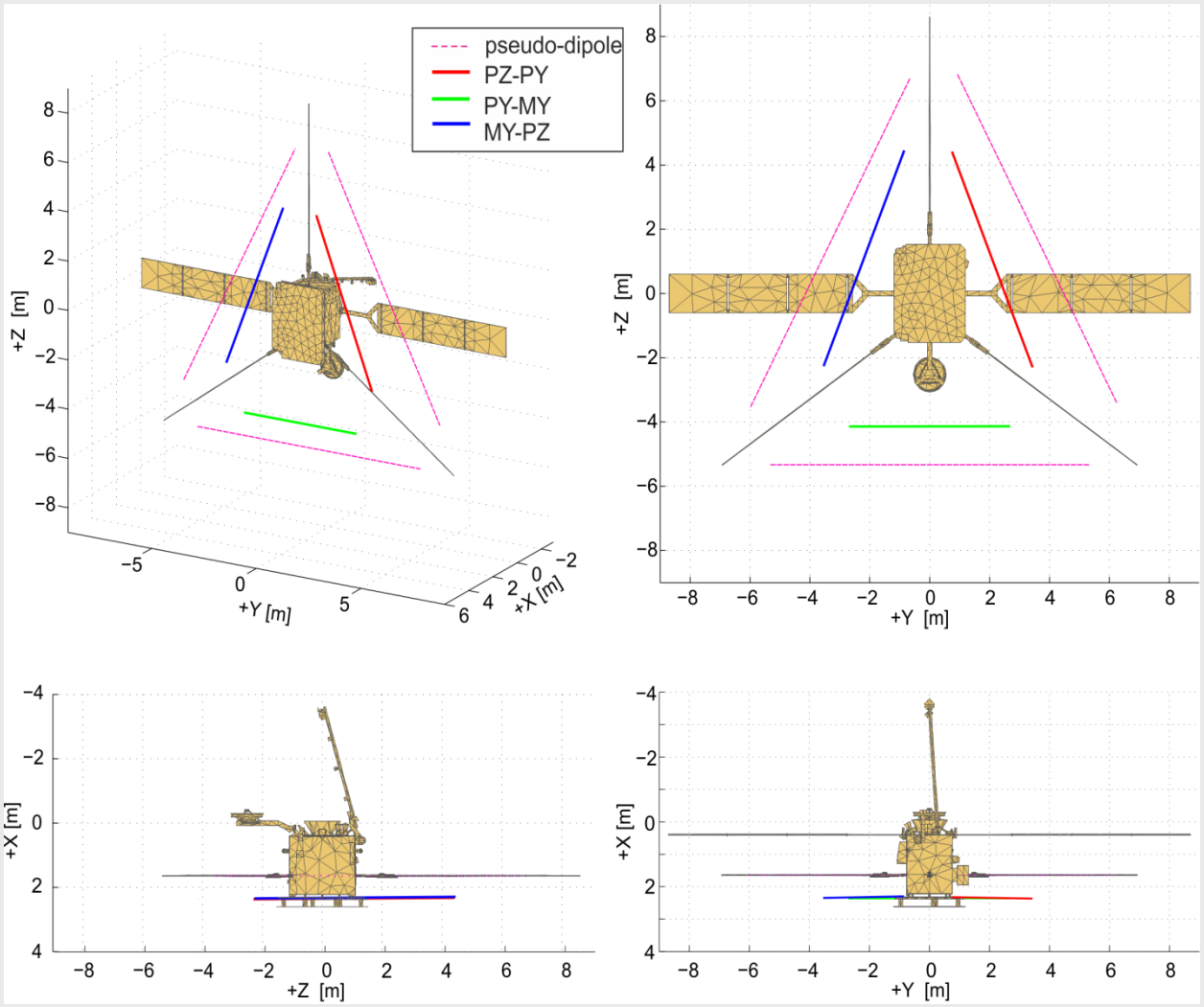

Effective length vectors at 300 kHz for a dipole configuration. The dipole effective vectors have been calculated from the effective vectors of monopoles.

Antenna capacitance matrix for monopoles

	Capacitance matrix (open port, pF)		
	PZ	**PY**	**MY**
PZ	71.6	-3.3	-3.3
PY	-3.3	72.9	-3.4
MY	-3.3	-3.4	72.9

Calculated open port capacitance matrix for the monopoles

The results can be compared with theoretical estimations (e.g. Macher & Oswald, 2011):

$$C = \frac{2\pi\varepsilon_0 l_A}{\ln\left(\frac{2l_A}{d}\right) - 1}$$

where l_A is the antenna length, *d is* the diameter of the antenna and e_0 is the permittivity of free space.

- For monopole antenna with l_A=6.5 m and the averaged diameter is *d*=0.0255 m the antenna capacitance after the equation is 69.1 pF.

- The small difference between theoretical estimations and the simulations can be explained that, in fact, the RPW monopole is a cone with a base diameter of 3.2 cm and a tip diameter of 1.9 cm while the equation is for cylindrical antennas.

Quasi-static results (300 kHz): loaded ports

- The loads at the ports can be represented by a local impedance matrix Z_L. The effect on the transfer matrix T is given by (Macher et al., 2007)

$$\boldsymbol{T} = (\mathbf{1} + \boldsymbol{Z}_A \boldsymbol{Z}_L^{-1})^{-1} \boldsymbol{T}^O = (\mathbf{1} + \boldsymbol{C}_A^{-1} \boldsymbol{C}_L)^{-1} \boldsymbol{T}^O$$

where $\boldsymbol{Z}_A$ and $\boldsymbol{C}_A$ are the antenna impedance and capacitance matrices and $\boldsymbol{T}^O$ is the open port transfer matrix which contains the open port effective length vectors as rows. The expression on the right is valid in the quasi-static frequency range. The load capacitance matrix $\boldsymbol{C}_L$ contains the base capacitances in its diagonal.

- We used the base (or stray) capacitance of each RPW antennas including receiver input, cables, and antenna mounting is 103 pF.

Antenna capacitances

		Monopole	Dipole
Antenna capacitance C_A	Length *L*	6.5	7.804
	radius *a*	0.015	0.015
	Ca for f << c/2πL	7.13E-11	4.13E-11
	C_A (pF) for f << c/2πL	**71.30**	**41.31**
Cstray	antenna Cstray	7.00E-11	
	preamplifier Cstray	3.30E-11	
	Stud Cstray	0.0	
	Cstray	1.03E-10	
	Cstray (pF)	**103.0**	**51.5**
$\Gamma = C_A / (C_A + C_S)$	**Γ for f << c/2πL**	**0.41**	**0.44**
Leff	min	4.71= 3.87*6.5/5.34	3.12
	max	5.37= 4.41*6.5/5.34	15.61
ΓLeff for f << c/2πL	min	**1.93**	**1.39**
	max	**2.19**	**6.95**

Table 4

M. Maksimovic, RPW Consortium Meeting #17EM Performances

Effective length vectors for open and loaded ports.

ANT	Open ports				Loaded ports ($\Gamma=C_a/(C_a+C_{str})=0.42$)			
	h_e, m	θ, deg	φ, deg	γ, deg	h_e, m	θ, deg	φ, deg	γ, deg
PZ	**4.41**	**9.1**	**-0.4**	**9.1**	**1.86**	**8.3**	**-0.4**	**8.3**
PY	**3.91**	**132.2**	**75.2**	**13.6**	**1.65**	**132.1**	**76.4**	**12.9**
MY	**3.91**	**132.3**	**-75.2**	**13.6**	**1.65**	**132.0**	**-76.3**	**12.9**
Dip. PZ-PY	**7.53**	**158.1**	**89.0**	**5.6**	**3.18**	**158.0**	**89.0**	**5.6**
Dip. PY-MY	**5.60**	**90.00**	**90.0**	**0.0**	**2.38**	**90.0**	**90.0**	**0.0**
Dip. MY-PZ	**7.53**	**158.2**	**-89.1**	**5.6**	**3.18**	**158.1**	**-88.9**	**5.6**

Effective length vectors for open port vs loaded ports. The calculation was done for total base capacitance 103 pF.

Far-field directivity in a quasi-static range

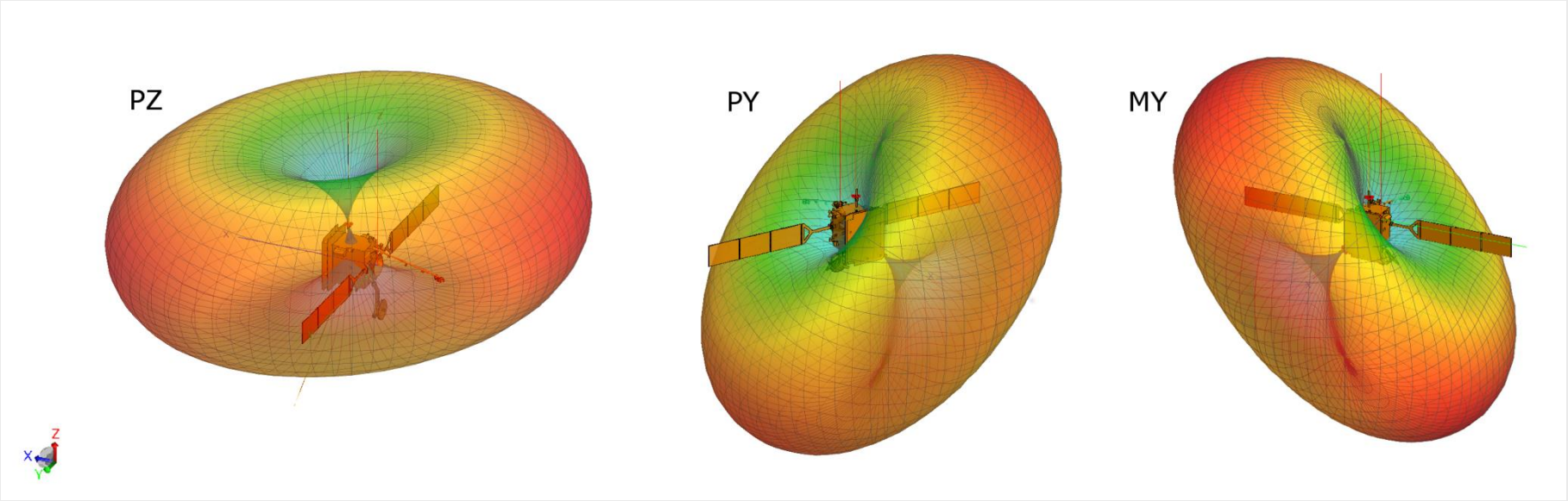

Far-field directivity pattern of the PZ, PY and MY antennas at 300 kHz. Color coding (in dB) indicates the total directivity

- The far-field directivity pattern of the RPW antennas in a quasi-static range have smooth toroidal shape

Thermal antenna bending

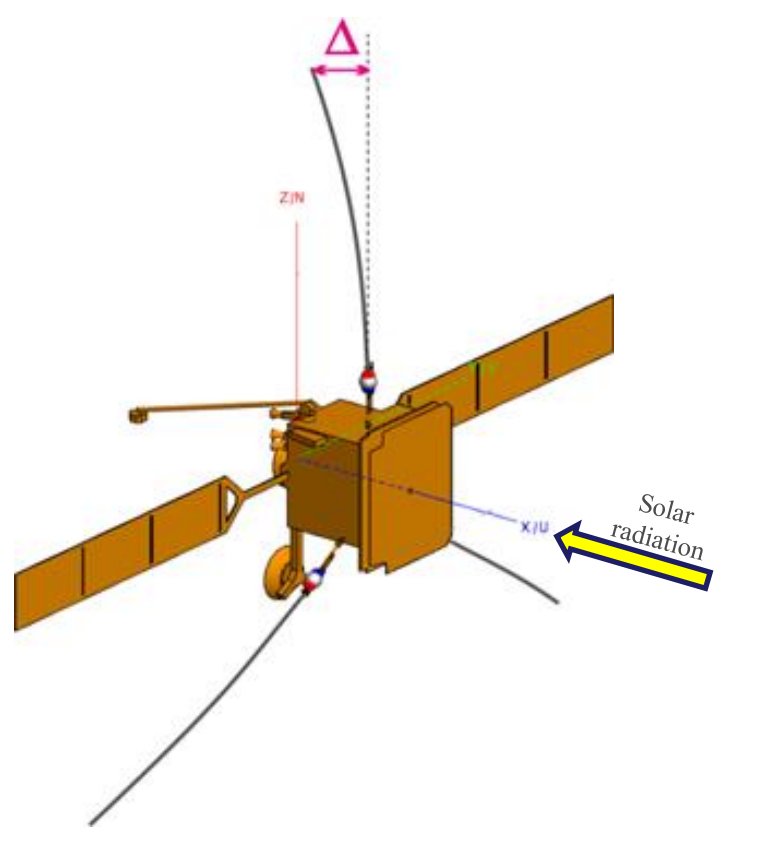

- Due to the attitude of the spacecraft, which is controlled in a way that the positive x-axis always faces toward the Sun, one side of each antennas will always face the Sun, while the other side will always be in the shadow.
- It is expected a large temperature gradient as result of the uneven illumination and thermal bending effect, which bends the antennas away from the Sun.
- The thermal bend estimated by CNES engineers can be more than 1.2 m at the distance of 0.22 AU from the Sun.
- Due to the thermal bending the antenna properties will be different compared to straight antennas.

Thermal antenna bending.

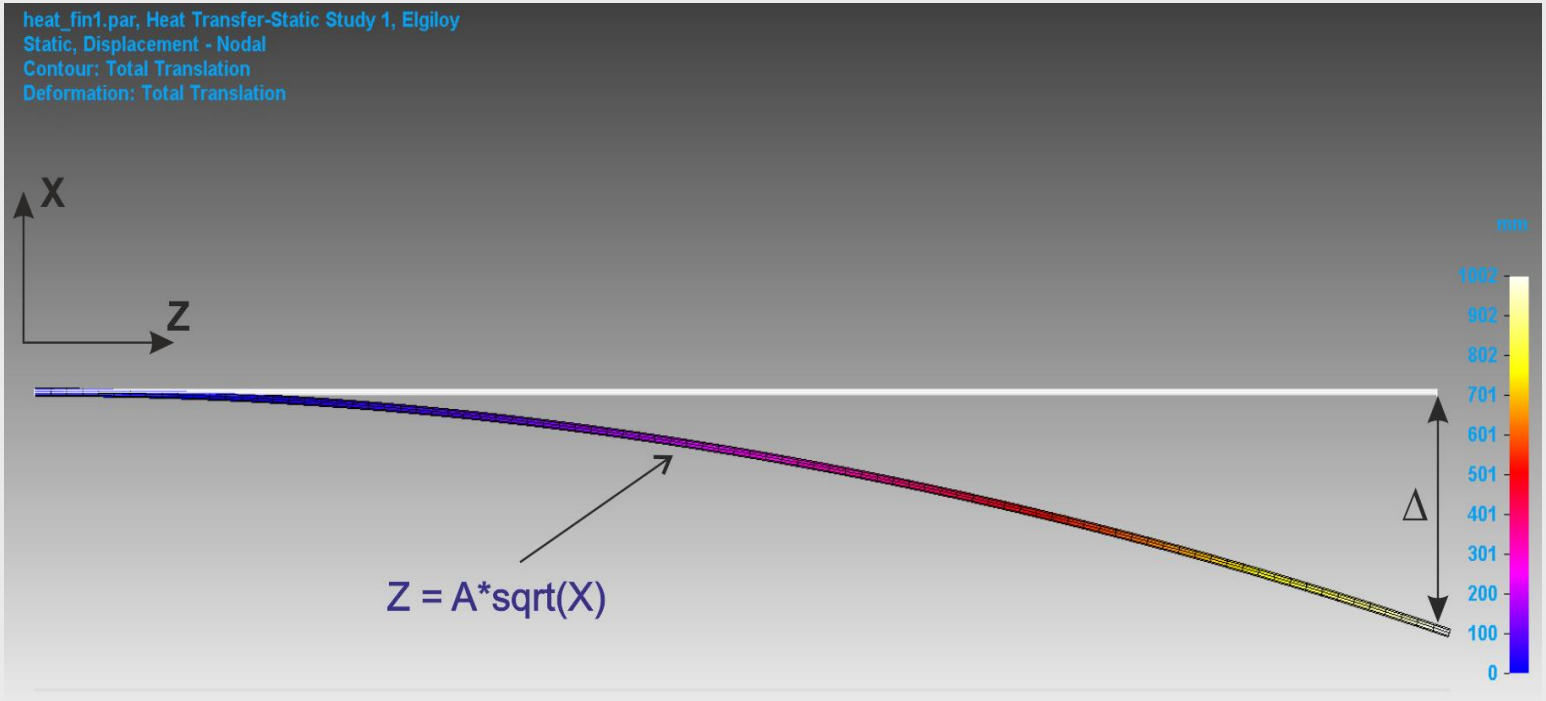

Bending of an unevenly heated cylindrical metallic (elgiloy) antenna. Δ shows offset of the antennas tip. Displacement of the deformed antenna stroke is coded by color. The shape of the bended antenna in XZ plane can be approximated as $Z = A\sqrt{X}$, where the coefficient A depends on the heat flux due to solar radiation.

Effective antenna vectors for different thermal bends

Tip offset	Effective antenna vectors											
	PZ				PY				MY			
Δ, m	h_e, m	θ, deg	φ, deg	γ, deg	h_e, m	θ, deg	φ, deg	γ, deg	h_e, m	θ, deg	φ, deg	γ, deg
0.0	4.41	9.1	-0.4	9.1	3.91	132.3	75.2	13.6	3.91	132.2	-75.2	13.6
0.1	4.41	8.7	-0.4	8.7	3.91	132.3	75.8	13.3	3.91	132.3	-75.8	13.2
0.2	4.41	8.4	-0.4	8.4	3.91	132.4	76.3	13.0	3.91	132.4	-76.2	13.0
0.3	4.41	8.1	-0.5	8.1	3.9	132.5	76.7	12.7	3.9	132.4	-76.7	12.7
0.4	4.4	7.7	-0.5	7.7	3.89	132.6	77.2	12.5	3.89	132.5	-77.2	12.5
0.5	4.4	7.4	-0.5	7.4	3.88	132.7	77.7	12.2	3.89	132.6	-77.7	12.2
0.6	4.39	7.0	-0.5	7.0	3.87	132.7	78.2	12.0	3.88	132.7	-78.2	11.9
0.7	4.38	6.7	-0.5	6.7	3.86	132.8	78.8	11.7	3.87	132.7	-78.7	11.7
0.8	4.38	6.4	-0.6	6.4	3.86	132.9	79.3	11.5	3.86	132.8	-79.3	11.4
0.9	4.37	6.0	-0.6	6.0	3.85	133.0	79.8	11.2	3.86	132.9	-79.8	11.2
1.0	4.37	5.7	-0.6	5.7	3.85	133.0	80.3	11.0	3.85	133.0	-80.3	10.9
1.1	4.37	5.3	-0.7	5.3	3.84	133.1	80.9	10.7	3.85	133.0	-80.8	10.7
1.2	4.37	5.0	-0.7	5.0	3.84	133.1	81.4	10.5	3.84	133.1	-81.4	10.5
1.3	4.37	4.6	-0.8	4.6	3.84	133.2	82.0	10.3	3.84	133.1	-81.9	10.2
1.4	4.37	4.2	-0.9	4.2	3.83	133.2	82.5	10.1	3.84	133.2	-82.5	10.0
1.5	4.37	3.9	-0.9	3.9	3.83	133.3	83.1	9.9	3.83	133.2	-83.1	9.8

The effective antenna vectors for different thermal bends (Δ) of the antennas.

Effective antenna vectors for different thermal bends

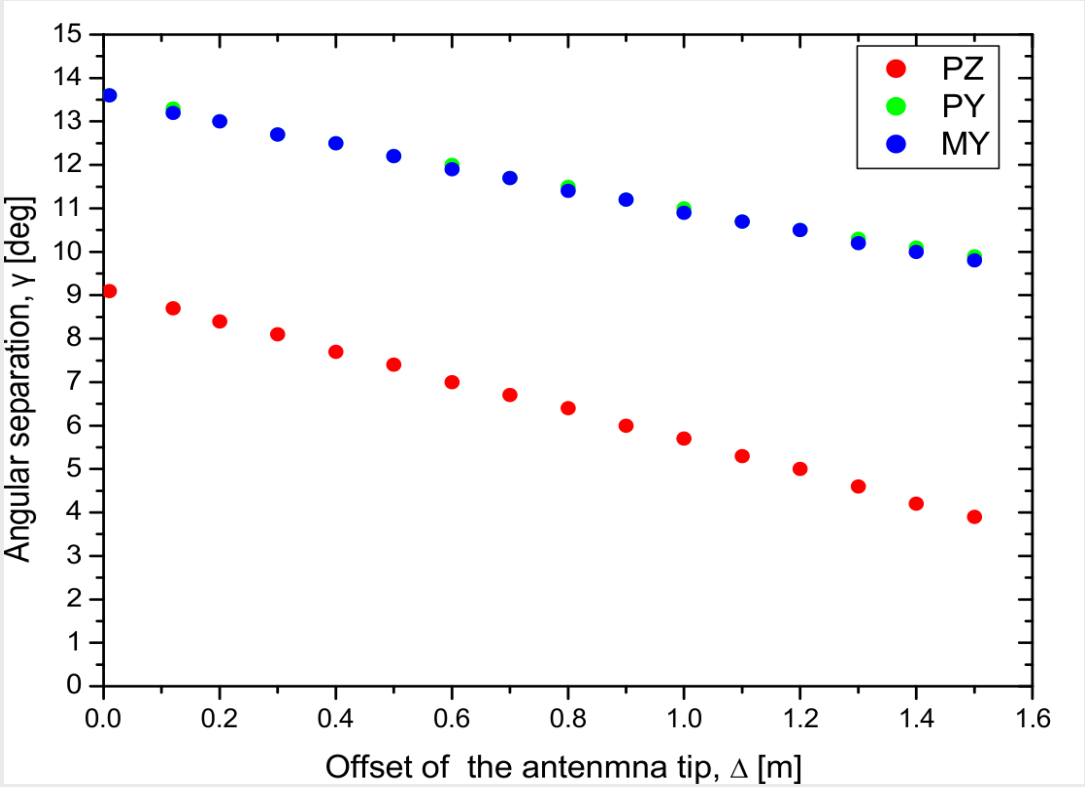

Dependence of the angular separation γ between the effective antenna vector and the real antenna rods is shown for different offsets of the antenna tip Δ.

- The tilt of the effective length vector is decreased from 9.1°,13.6°,13.6° up to 3.9°, 9.9° and 9.9° for the Δ = 1.5 m.
- The decreasing of the effective length (h_e) is small from 4.41 to 4.37 m for PZ antenna and from 3.91 to 3.83 for PY and MY antennas.

Dependence on the solar panel orientation

- We have also simulated the antenna reception properties for different position of the rotatable solar panels. The panels can be turned up to 45 deg. out of the vertical position during different phases of the spacecraft mission.
- *No significant influence of the solar panel rotation on the resulting effective antenna vectors has been found*.

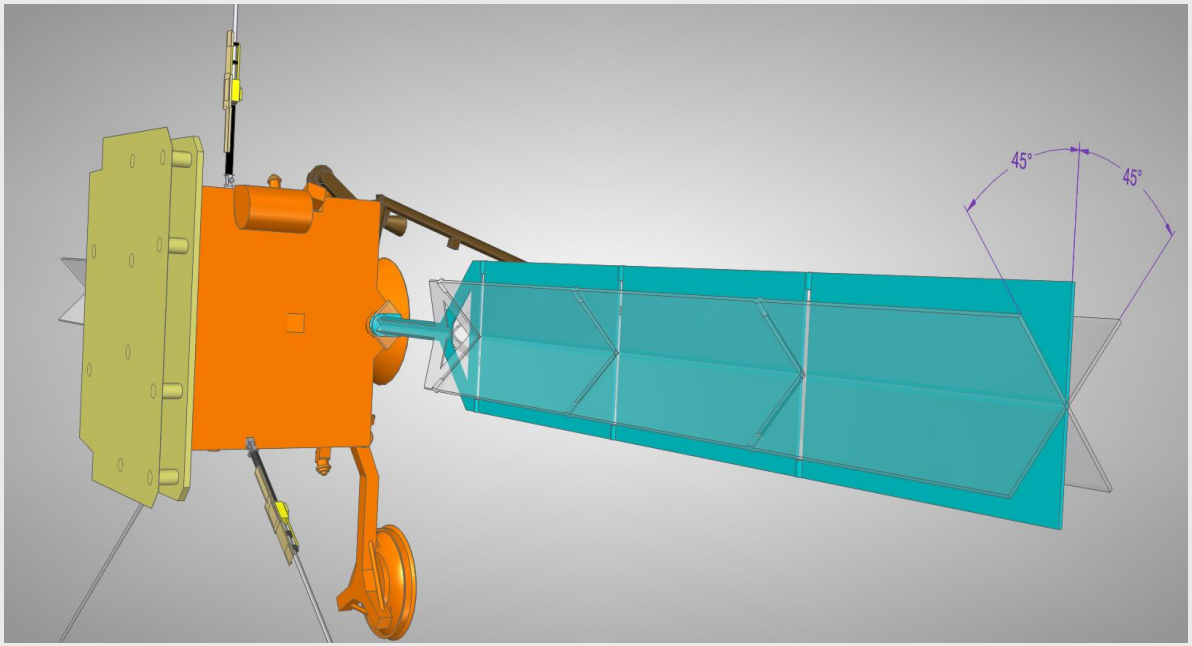

High-frequency characteristics

- The directivity patterns and the impedances of the antenna have been also simulated up to frequencies of 16 MHz.
- Far-field directivity patterns have smooth toroidal shape from quasi-static range up to ~9 MHz
- For the higher frequencies the patterns are strongly frequency dependent. It has a complex shape with several lobes as the patterns.

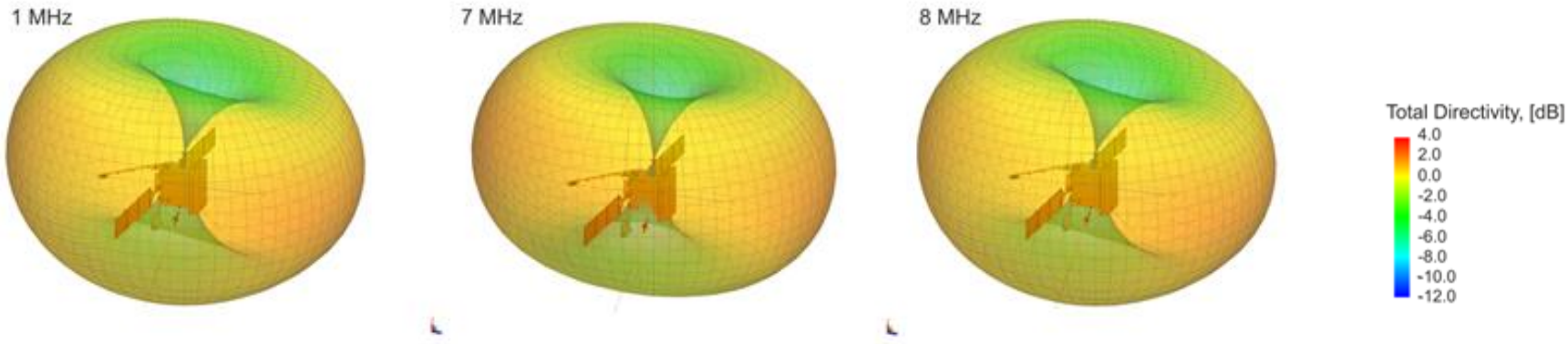

Far-field directivity patterns of **PZ** antenna for frequency range 1MHz – 8 MHz. Color coding (in dB) indicates the total directivity

High-frequency characteristics

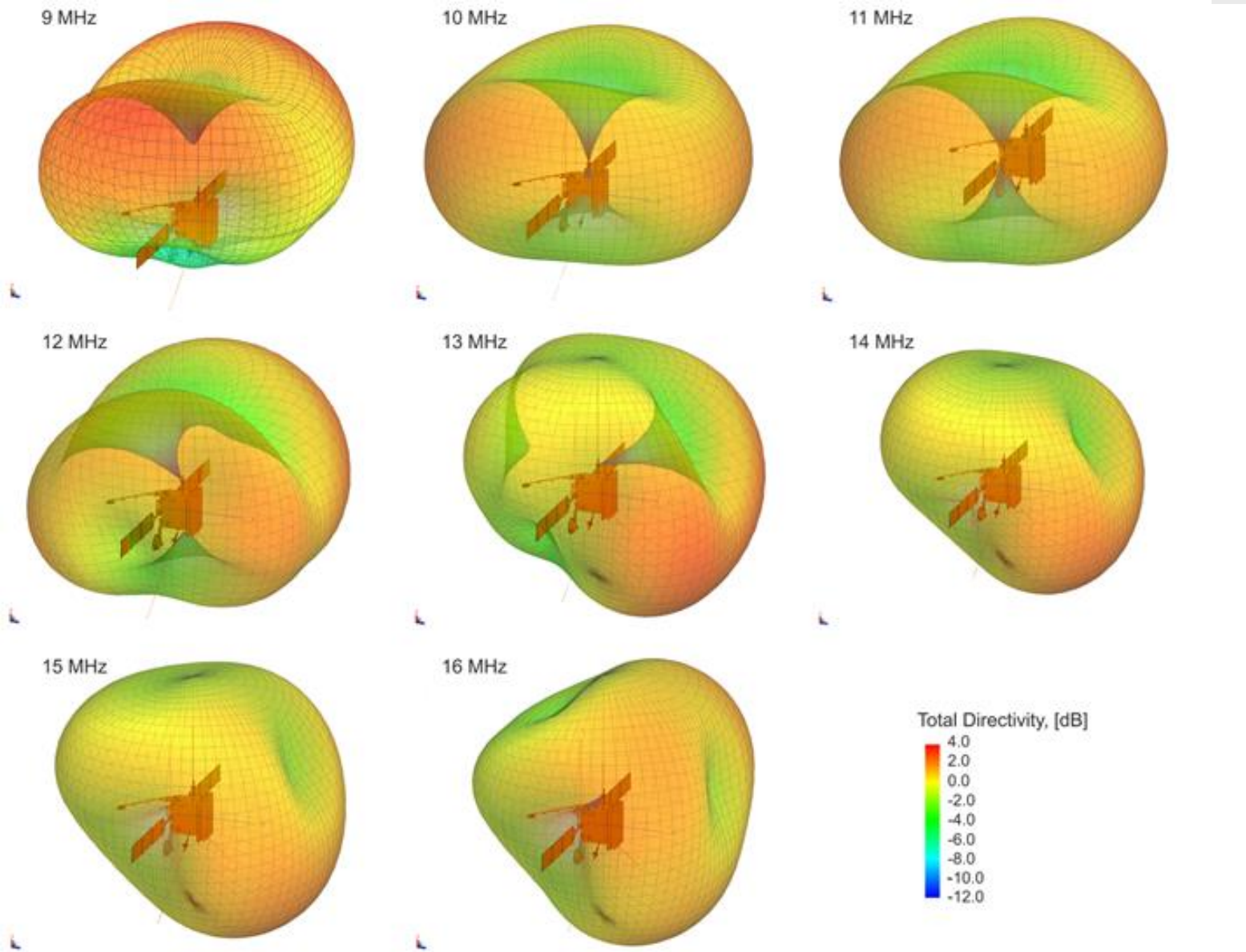

Far-field directivity patterns of **PZ** antenna for frequency range 9MHz – 16 MHz

Antenna impedances.

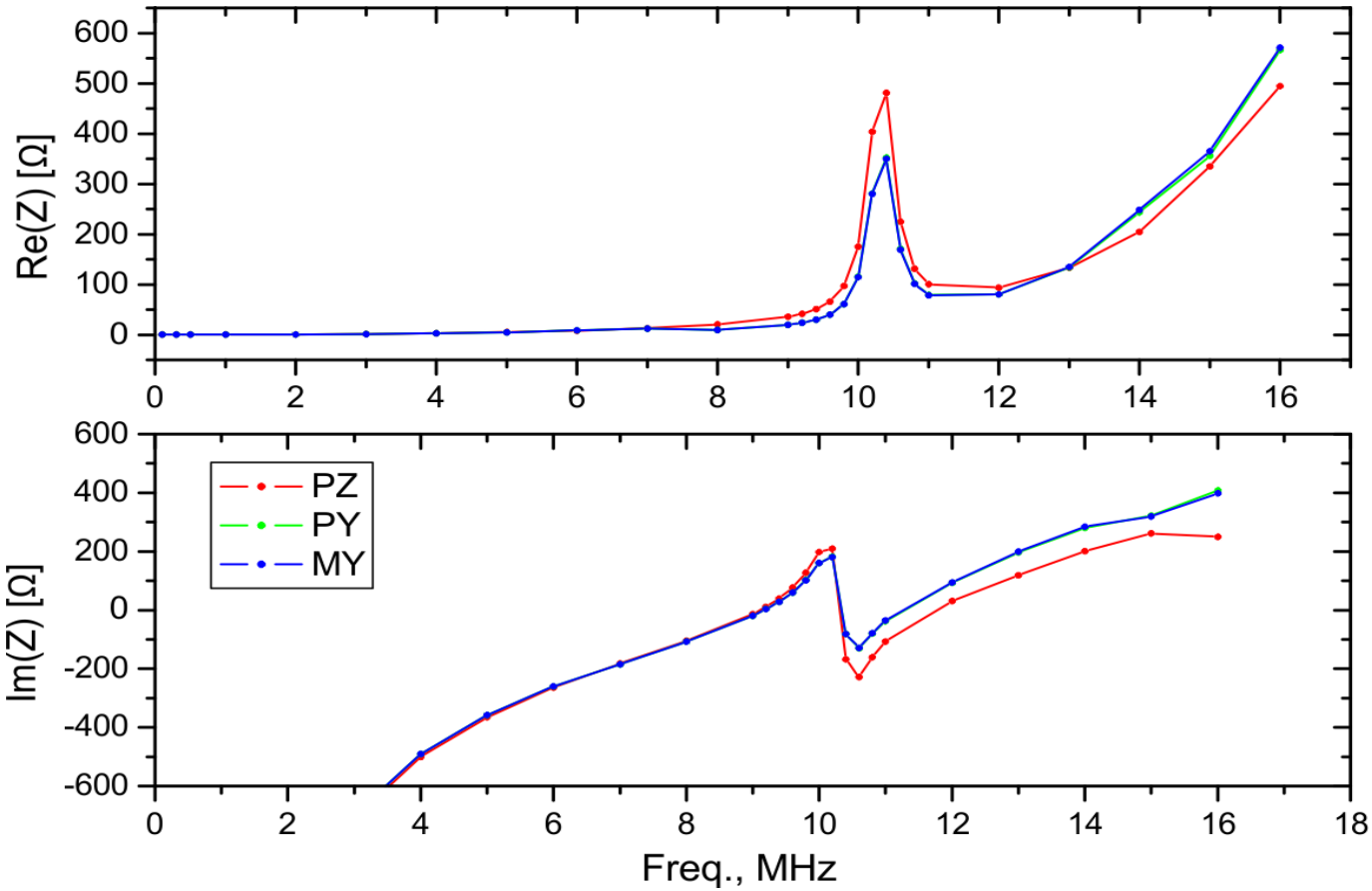

Frequency dependent antenna impedances. Antenna resonance at ~10.3 MHz is clearly seen, when the imaginary part of the impedance has a zero crossing.

2. Rheometry measurements

- **Rheometry**. The method is based on electrolytic tank measurements where the scaled model is immersed in a water-filled tank.
- Metal plates are connected to a signal generator forming a large capacitor with homogeneous electric field in the tank.
- Voltmeter is connected to the antenna terminal and the induced voltages are measured depending antenna orientation.
- This technique allows us to determine the effective length vectors of the antennas in the quasi-static frequency range.

- The rheometry method have been applied for calibration of the antennas onboard Cassini-RPWS, Interball/POLRAD, STEREO/WAVES, Resonance and Juno missions.

Scale model

- The Rheometry measurements were performed using the 1:50 scaled gold platted model of the Solar Orbiter

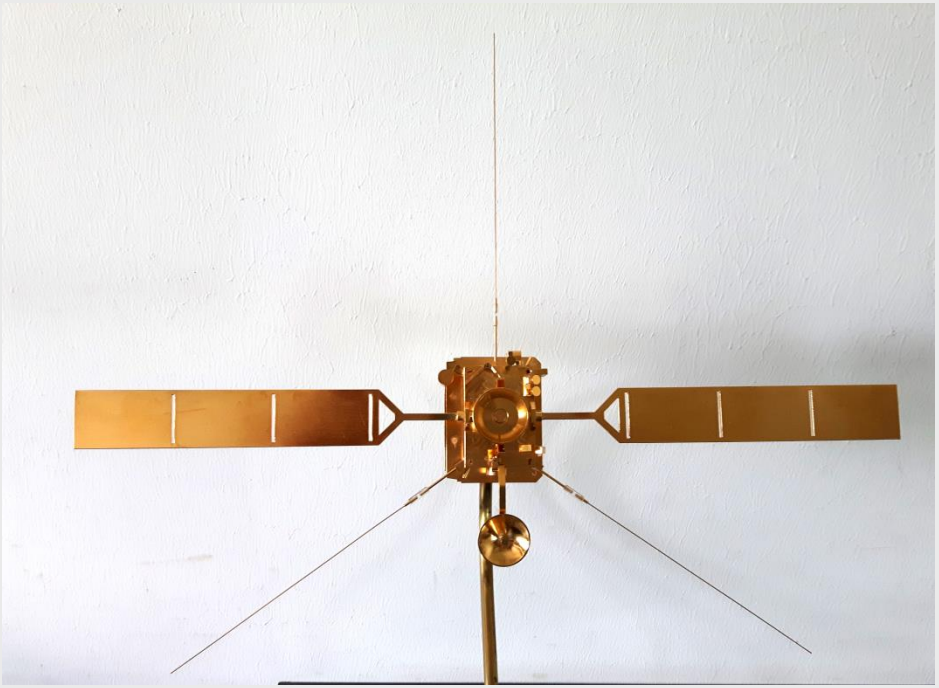

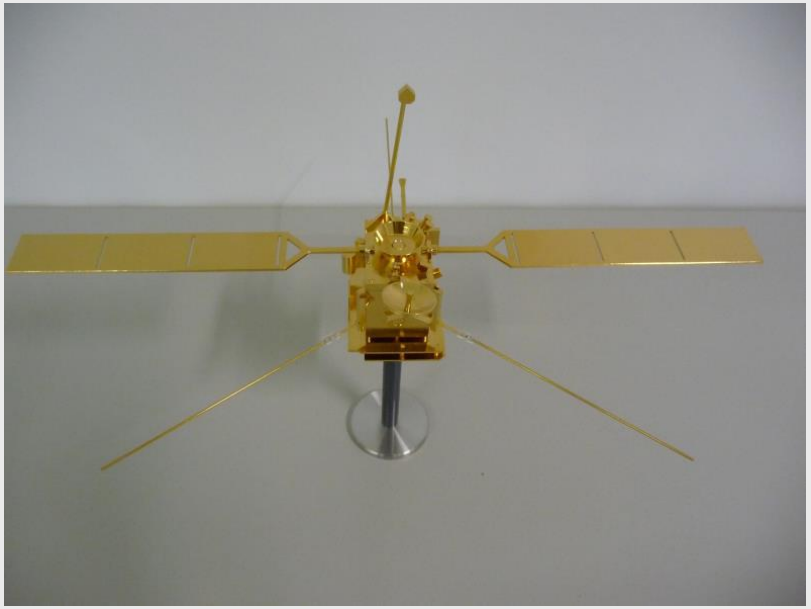

Solar orbiter model

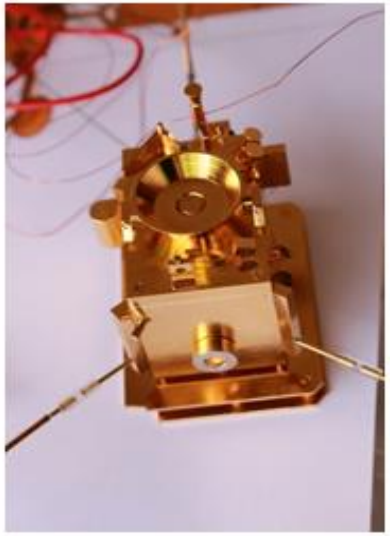

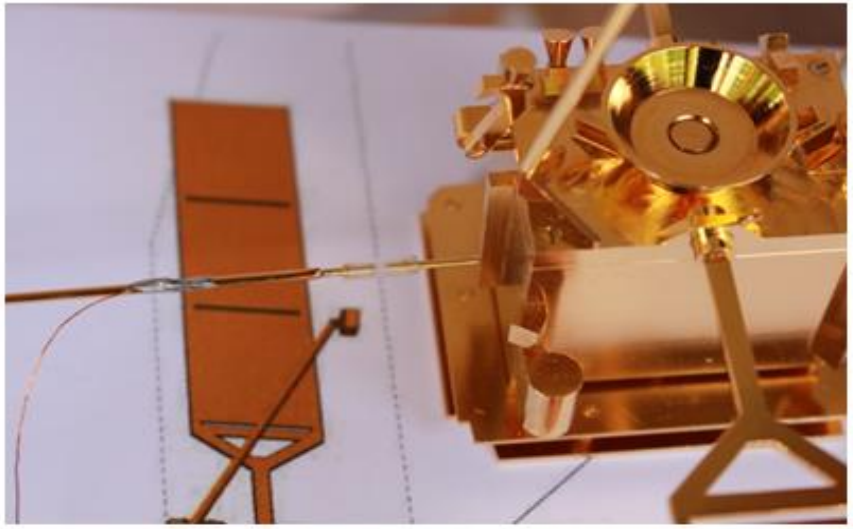

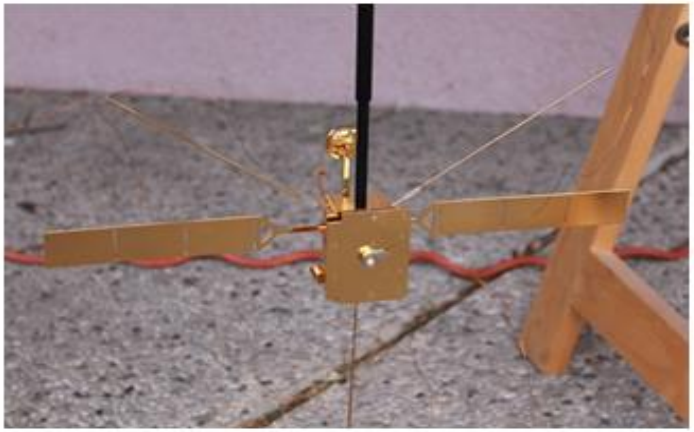

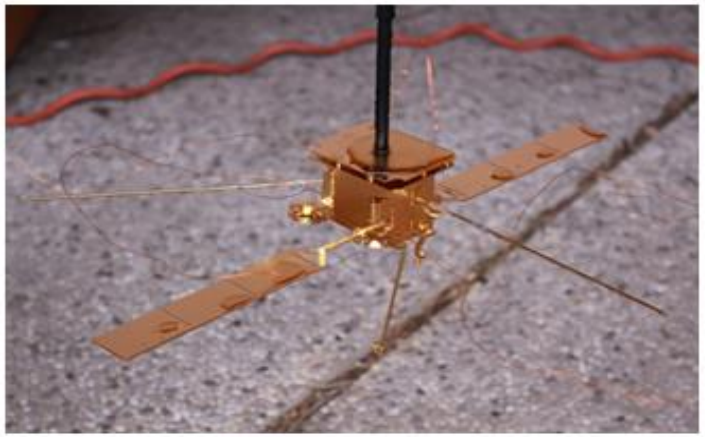

RPW antenna for Rheometry

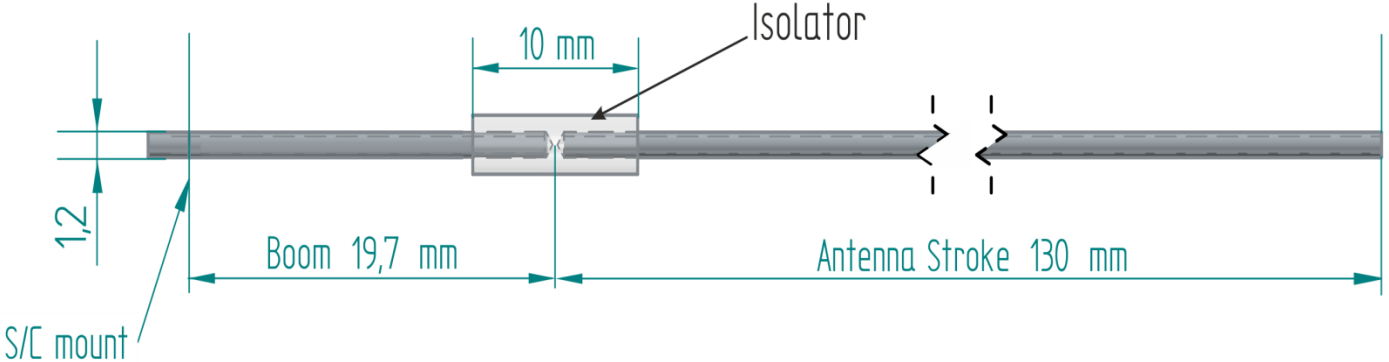

RPW antennas for the rheometry experiment. The boom and the antenna stroke is separated by a plastic isolator.

Rheometry measurements

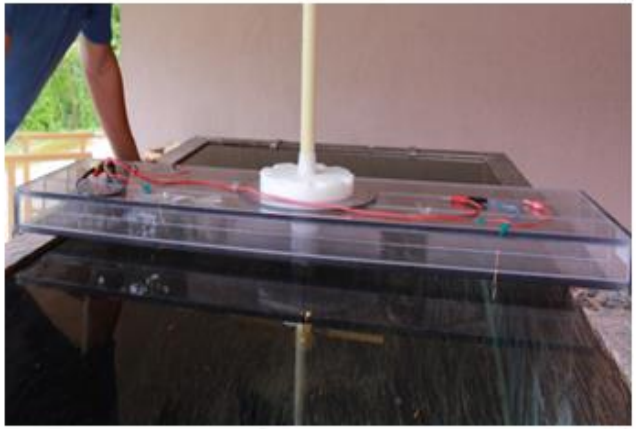

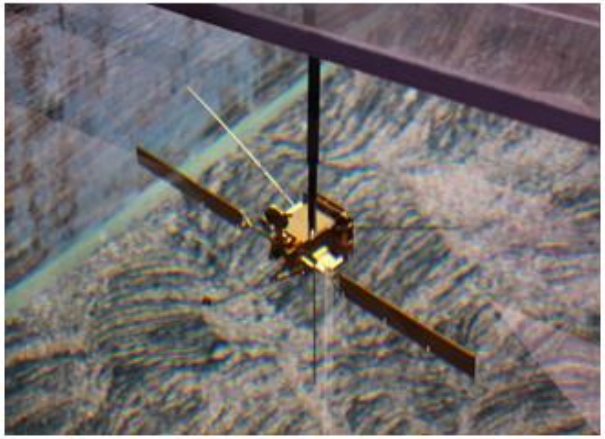

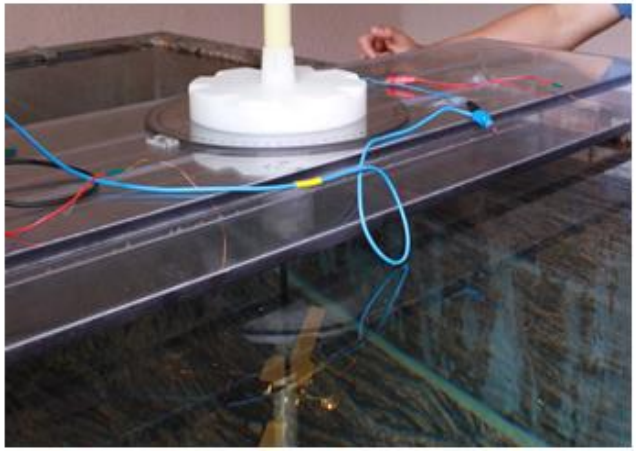

Results of rheometry measurements for open port

ANT	Mechanical antennas			Effective antenna vectors			
	h, m	θ, deg	φ, deg	h_e, m	θ, deg	φ, deg	g, deg
PZ	6.5	0.0	0.0	4.58	8.4	-5.1	8.4
PY	6.5	125	90	4.12	132.8	75.0	14.1
MY	6.5	125	-90	4.15	133.5	-75.9	13.8
	Pseudo dipoles			Effective vectors of dipoles			
Dip. PZ-PY	11.53	152.5	90	7.91	157.9	87.8	5.5
Dip. PY-MY	10.65	90.0	90	5.89	90.0	89.6	0.4
Dip. MY-PZ	11.53	152.5	-90	7.89	158.4	-88.4	5.9

Effective length vectors of PZ, PY and MY monopoles and PZ-PY, PY-MY and MY-PZ dipoles compared with physical position of the RPW antennas. h is antenna length, θ is colatitude and φ is azimuth angle. The angle γ is the angular separation between effective antenna vector and real antenna rod. The dipole effective vectors have been calculated from effective vector of the monopoles.

Rheometry measurements for loaded port

ANT	Mechanical antennas			Effective antenna vectors			
	h, m	θ, deg	φ, deg	h_e, m	θ, deg	φ, deg	g, deg
PZ	6.5	0.0	0.0	1.94	7.6	-5.3	7.6
PY	6.5	125	90	1.74	132.6	76.1	13.2
MY	6.5	125	-90	1.75	132.3	-77.0	12.5
Dip. PZ-PY	11.53	152.5	90	3.35	157.7	87.7	5.3
Dip. PY-MY	10.65	90.0	90	2.51	89.9	89.6	0.4
Dip. MY-PZ	11.53	152.5	-90	3.34	158.2	-88.3	5.8

Results of the rheometry measurements for loaded ports. The calculation was done for total base capacitance 103 pF.

Numerical simulations vs. rheometry

Effective length vectors from numerical simulations and rheometry measurements for open ports.

ANT	Numerical simualtions				Rheometry measurements			
	h_e, m	θ, deg	φ, deg	γ, deg	h_e, m	θ, deg	φ, deg	γ, deg
PZ	4.41	9.1	-0.4	9.1	4.58	8.4	-5.1	8.4
PY	3.91	132.2	75.2	13.6	4.12	132.8	75.0	14.1
MY	3.91	132.3	-75.2	13.6	4.15	133.5	-75.9	13.8
Dip. PZ-PY	7.53	158.1	89.0	5.6	7.91	157.9	87.8	5.5
Dip. PY-MY	5.60	90.00	90.0	0.0	5.89	90.0	89.6	0.4
Dip. MY-PZ	7.53	158.2	-89.1	5.6	7.89	158.4	-88.4	5.9

- Rheometry measurements are in good agreement with numerical calculations.
- The effective antenna lengths from the numerical simulations are about 4-5% shorter than lengths from the rheometry measurements. The reason of this difference, that the real antenna is mounted on the 1 m boom with metallic thermal shield and, therefore, the part of each antenna (0.42m) is partially in the shadow of these conductive thermal shields. Due to small size of the scaled model it was not possible to reproduce these thermal shields in the hardware spacecraft model. Therefore the effective antenna length in numerical simulation, which includes thermal shields, is shorter than the effective lengths obtained from the rheometry measurements.

Summary

- The reception properties of the RPW antennas have been studied using the numerical simulations and experimental measurements.
- The numerical simulation have been performed to define the effective length vectors and the antenna impedance in a frequency range from the quasi-static up to 16 MHz. The effective antenna vectors ($\mathbf{h_e}$) tilted towards +X (sun) axis. Directivity patterns have toroidal shape up to frequency ~9 MHz. For the higher frequencies the pattern become more complex.
- The influence of the thermal bending of the antennas on resulting effective antenna vectors have been studied. The thermal bend decreases the tilt of the $\mathbf{h_e}$ from the physical antenna position. We provided $\mathbf{h_e}$ for different thermal deformations which will correspond to different orbital phases of the Solar Orbiter mission.
- The antenna effective vectors have been also calculated by means of Rheometry technique which uses a down-scaled gold-plated model of the spacecraft. The obtained results are in a good agreement with the numerical simulations.